Biophysical Chemistry 125 (2007) 13 – 23

Biophysical Chemistry

http://www.elsevier.com/locate/biophyschem

Photophysics of ANS. II: Charge transfer character of near-UV absorption and consequences for ANS spectroscopy

William Kirk

Mayo Foundation, Rochester, MN 55902, USA

Received 18 January 2006; received in revised form 26 July 2006; accepted 31 July 2006

Abstract

We continue our investigation of the photophysics of 1,8-anilinonaphthalenesulfonate in protein and solvent systems. In this report, we concentrate on the nature of the excited states as observed in UV spectra. We develop a fairly general formalism for handling the coupled transitions we observe in the *partial* systems aniline and naphthalene. We assign one of the near-UV transitions, which is more clearly discernible in congeners of 1,8-ANS, but still present in 1,8-ANS as we postulate it, to a charge-transfer band. The other transition is from aniline itself. The expected energies of these now coupled bands in anilinonaphthalene and ANS are calculated, and the transition dipole moment for these transitions is derived.
Published by Elsevier B.V.

Keywords: Charge transfer transition; Exciton theory; ANS electrochemistry

Research using 1,8-anilinonaphthalenesulfonate is often focused on its ability to 'probe' a supposedly hydrophobic or amphipathic environment [1]; for a review of general ANS photophysics, see [2]. Besides merely exploiting the spectral changes observed in ANS upon binding to a protein or molten globule, it is conceivable that the actual spectral data, e.g., wavelength of emission, quantum yield, etc., could yield more detailed information about the nature of the interaction and/or binding site. Progress has been made in this direction recently with the intrinsic probe fluorescence of *tryptophan* residues [3]. There is no reason to think that a similar understanding of ANS photophysics is impossible. This paper is a contribution to that end. We warn the reader at the outset that we will employ several models of 'mixing' of transitions, at different levels of refinement, to attempt an explanation of several features of the UV–Vis spectroscopy of 1,8-ANS and related anilinonaphthalenes. But we keep all the formalism confined within the domain of spectroscopy, of actual spectra, and attempt no 'quantum chemical' calculations, as that term is currently understood, because without addressing some of the issues we present herein first, there is no justification for doing any such calculation at any level below the complete *ab initio* with doubly excited configurations in the basis-set plus correlation corrections on ANS itself, including all 40 electrons on the sulfonate group—a rather formidable task—just to obtain the ground state accurately. There would be no justifiable simplification. It also means one would have to be able to complete this task accurately up to the fourth excited state, as we demonstrate below.

1. Theory and calculations

1.1. Aniline and naphthalene molecular orbital theory

We present a brief account of the molecular orbital (MO) theory of aniline and naphthalene systems, recognizing that it is a simplified model at best. Nonetheless, some aspects of these considerations do seem to be accurate representations of the actual photophysics of this and related systems [4]. A few of the important molecular orbitals for aniline and naphthalene are shown in Fig. 1, together with their conventional (Mulliken) and 'natural' (cf. Butler [5]) group designations. The 'natural' system designates each irreducible representation (irrep) in terms of the SO_3, or three-dimensional angular momentum group irrep from which it is descended. Thus, an irrep labelled $|1>_G$ in the natural system for the group 'G', possesses, when brought back up to the level of a single hydrogenic electron wave function, 1 unit of angular momentum. The irrep $|0>$ is the pure scalar irrep, and

---

E-mail address: kirk.william@mayo.edu.

0301-4622/$ - see front matter. Published by Elsevier B.V.
doi:10.1016/j.bpc.2006.07.017

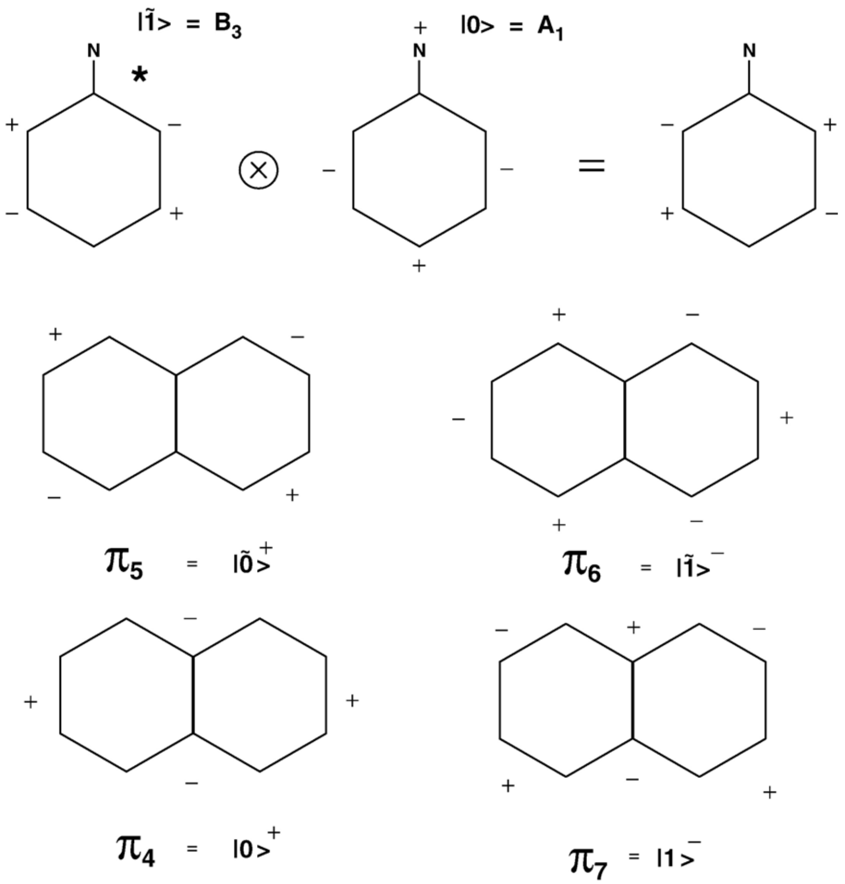

Fig. 1. Schema of the highest occupied and lowest unoccupied molecular orbitals for aniline (a) and naphthalene (b), showing conventional (Millikan) and 'natural' nomenclature of the group-theoretical irrep labels. As these are graphical representations of wave functions, the '+' and '−' signs connote effective electronic amplitude increments or decrements relative to some zero, like lobes of orbitals with the +/− signs as relative phases, between these are then the *nodes* of the wave function, and one can imagine the signs oscillating at a frequency of E_{orb}/h^{-} (E_{orb} is the energy of the orbital); an electronic *state density*, being the complex conjugate of the amplitude times the amplitude itself, does not oscillate, but a transition density *does*, at the difference frequency $(E_{\mathrm{orb},1}-E_{\mathrm{orb},2})/h^{-}$ of light absorption.

irreps designated with a tilde, ~, have an additional 'odd' characteristic. That is, they are products of the underlying irrep $|\mathbf{j}>x|^{\sim}0>$, where $|^{\sim}0>$ is a one-dimensional irrep, like $|0>$, but which has polar-vector properties under reflections.

In Fig. 1 then, aniline is seen to have its lowest lying transition from $\mathbf{A}_{2u}$ to $\mathbf{B}_{1u}$ which yields a transition with a very weak dipole moment (as observed), possibly strong quadrupole moment, and at least partial $n\rightarrow\pi^*$ character (if account is taken of the dispersal of electron density from the amino nitrogen).

For naphthalene, the ^1L_b transition is a linear combination of $\pi_4\rightarrow\pi_6$ and $\pi_5\rightarrow\pi_7$ transitions, which means it is polarized along the long axis, but in such a way that the contributions nearly cancel, so that it is very weak in the parent molecule, naphthalene itself. The ^1L_a transition is mostly $\pi_5\rightarrow\pi_6$ which makes it polarized along the short axis, but it is generally much stronger in the parent naphthalene. In *1-amino* naphthalenes, the ^1L_a transition is shifted to the red, so that it is now lower lying than the ^1L_b—which is the lower lying transition in the parent system (and in naphthalene-1-sulfonic acid, for example, as well). In 1-amino naphthalenes, one can well imagine that the positive pole of the ^1L_a transition density lies on the side of the amino group (stabilized perhaps by the 'valence structure' $>=\mathrm{NH}_2^+$). This conjecture can be readily supported by observing the absorption spectrum of *1-sulfo, 2-anilino*-naphthalene, in comparison with *1-anilino, 2-sulfo*-naphthalene (Fig. 2A), wherein both naphthalenic bands appear to be 'forbidden,' in other words, the valence polarization readily envisioned between *ortho* sulfonate and amino groups, which would lead to charge flow from the nitrogen onto the sulfo, is compatible with the transition density of the ^1L_a transition when the amino group is in the "1" and the sulfo the "2" position, but not vice versa. We suggest that in naphthalenic L_a transitions, there is thus net electron flow from '1' to '2'. The polarizing effect of amino should be enhanced by substitution to anilino. In addition, the presence of sulfonate *and* anilino at 1 and 8 should be mutually reinforcing and therefore increase the transition density associated with ^1L_b (by stabilizing charge separation along the long axis); they should also cause the transition to shift to the red. Thus, for example, in 1,8-*amino* naphthalene sulfonate, it is difficult to unambiguously separate the two transitions (Fig. 2B), and in 1,8-ANS, the two transitions are much closer in intensity than in, e.g., 1,2 ANS or naphthalene (cf. Ref. [6]).

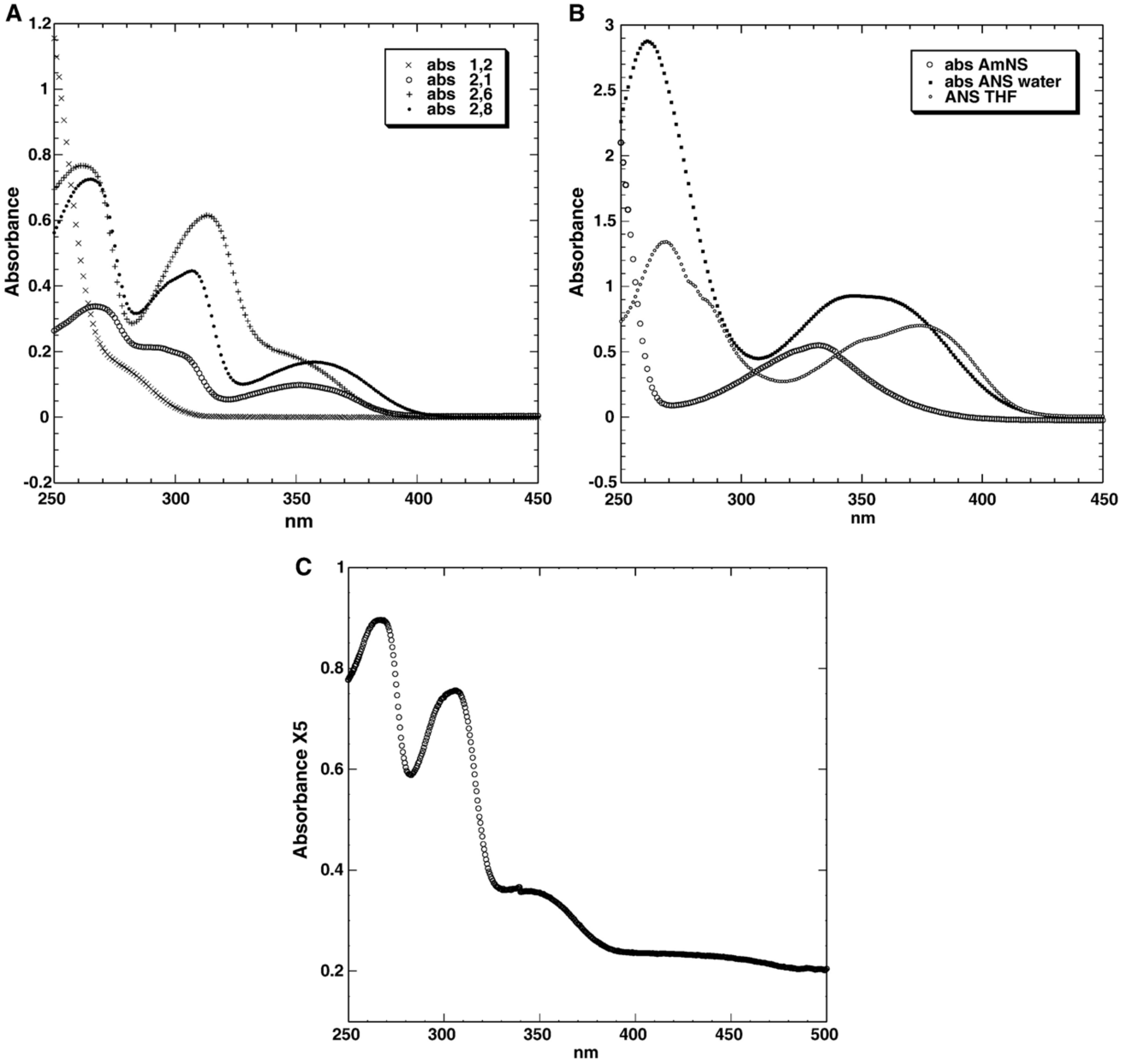

Fig. 2. (A) Absorbance spectra of ANS congeners in water: 1,2 ANS, ~2 mg/100 ml (~66 μM). (×××); 2,1 ANS, ~1 mg/200 ml (~17 μM) (□□□); 2,8 ANS, 1 mg/100 ml (~33 μM) (◎◎◎); and 2,6 ANS, ~1 mg/100 ml (~33 μM) (+++). The numbering system is such that the lowest number refers to the *sulfo* and the higher number to the *anilino* position on the naphthyl ring. (B) AmNS, 90 μM; ANS in water, 185 μM ; ANS in THF, ~2 mg/100 ml. (C) AnN in water, ~3 mg/l (~13 μM near saturated).

1.2. Charge transfer energetics: Electrochemistry and solvation

But there is another feature in spectra of anilinonaphthalenes: there is a charge-transfer (CT) band. We designate the spectral feature appearing in most of the UV spectra of Fig. 2 as CT on the basis of the following observations, which comport with 'classical' indications dating back to Mulliken [7]. There are *two* bands in the region 250–290 nm for most of the naphthalenes shown in Fig. 2. *One* of these bands can be safely attributed to aniline itself. But the existence of a new band not present in either of the parent spectra is immediately indicative of a CT band. This is true even in 1,8-ANS, though it seems at first sight to have but one transition. As can be seen, however, if one dissolves ANS in THF as in Fig. 2B, what was one single band becomes partially resolved into two. Moreover, this new band has a significant oscillator strength and is vibrationally featureless, as Mulliken had predicted should be the case for CT bands. Lastly, we perform below a calculation of the energy of the band and can succeed in producing an expected CT transition energy in the observed region.

The scheme in Fig. 3A shows some of the energetics involved in this CT transition. First, there is the *ionization potential* of the aniline donor, and the *electron affinity* of the naphthalene acceptor. These are values from the *gas phase*. Next, there is the reorganization energy of the orbitals belonging to both donor and acceptor to accommodate a distribution of excess charge. This reorganization energy is

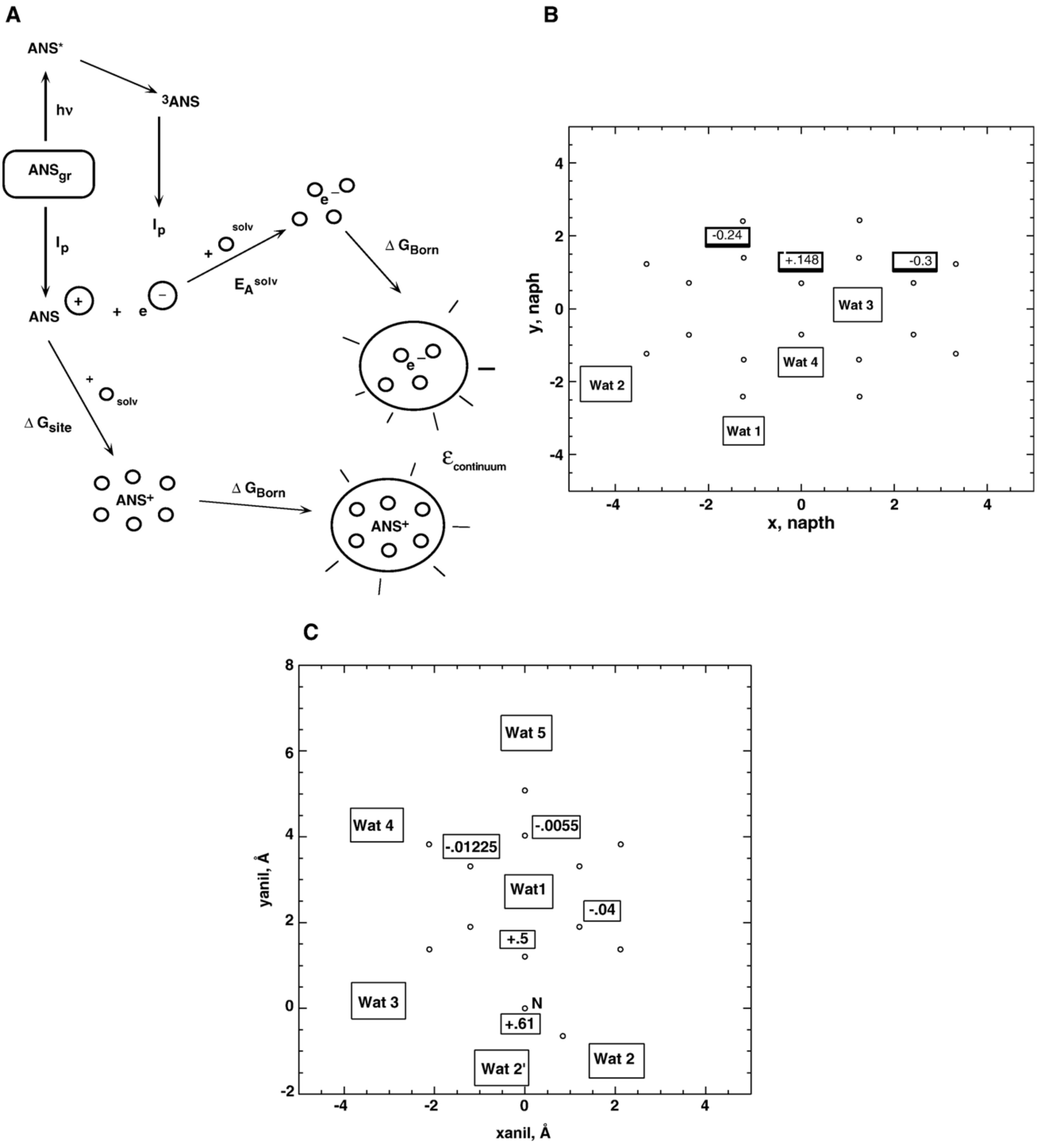

Fig. 3. (A) Schematic illustration of the sources of electrochemical work in the anilinonaphthalene system. Many more processes are included than we actually confront in this paper; they are more relevant in a later contribution. But we present them here because we calculate the aniline-to-naphthalene charge-transfer energy in this paper. (B) The naphthalene system, with the excess charges calculated via the Applequist polarizabilities. (C) The aniline system, with excess charge distribution. Coordinates are in Ångstroms.

included in the 'adiabatic' ionization energy (as opposed to the 'vertical' energy which includes only a minimal part of it—but is more constitutive of light-driven CT events). Then the incipient final state is decorated with nearest neighbor solvent molecules. An *inner sphere hydration energy* which we designate as *site-solvation*, is contributed by reorientation and repolarization of these adjacent water molecules. Lastly, the solutes and inner-sphere waters together form a cavity, which can be inserted into a dielectric continuum (since at some point the particulate nature of the solvent is 'washed out', and we are left with bulk solvation), and the corresponding *Born solvation energy* can be calculated. The Born term is given by $(e_0^2/2R)(1/\varepsilon-1)$ for a cavity of radius R.

The vertical ionization potential of aniline is 8.05 eV, the electron affinity of naphthalene is 0.15 eV. Thus, in gas phase, one requires $8.05-0.15=7.9$ eV of work to transfer an electron from aniline to naphthalene, with the minimum nuclear reorganization (the vertical energy). The addition of the sulfo group to the *meta* position in anilines was shown to decrease the pK_a of the amino by 0.3 units [8]. Thus, we can expect a similar approximately additive contribution to the electron affinity, decreasing the value by ~.03 eV. In addition, there is a change in the ionization potential in *naphthalene* (8.15 eV) due to the existence of the amino. This would be an important consideration for possible electron transfer quenching of the naphthyl excited state (see our next contribution). We discuss this subject matter here because the type of calculation involved concerns us primarily in *this* contribution. Essentially, we again assume additivity, in that changes in the redox potential in going from naphthalene to amino naphthalene, or, for that matter, from benzene to aniline, are both roughly −1.16 eV (all these values are from Murov et al. [9]). We assume here that, for the ionization of ANS (from the naphthyl ring), we shall subtract 1.16 eV from the value for naphthalene and subtract another 3 kJ/mol for the presence of the sulfo group (that is, $2.303RT\log(0.3)$).

The charged species must then be solvated. The monopolar and dipolar polarizabilities of Applequist [10] were employed to generate a likely excess partial charge distribution on naphthalenide and anilinium carbons and nitrogen after the CT event. We employed a monopole polarizability of 0.5 (atomic units) for the nitrogen.

The Applequist model generates induced partial charges on the atoms of the system according to the following coupled equations for the charges and dipole moments in terms of the monopole and dipolar polarizabilities (σ and α, respectively), field $\boldsymbol{E}_i$ and potential ϕ_i at each atom:

$$q_i = -\sigma_i \phi_i; \tag{1a}$$

$$\mu_{is} = \alpha_{is} E_{is} \tag{1b}$$

$$\phi_i = \sum_j \left(T_{i0jo} q_j + \sum_i T_{i0jt} \mu_{jt}\right) \tag{1c}$$

$$E_{is} = \sum_j \left(T_{isjo} q_j + \sum_i T_{isjt} \mu_{jt}\right) \tag{1d}$$

where $T_{i0j0} = \boldsymbol{r}_{ji}^{-1}$; $T_{i0jt} = r_{ji}^{-3}\ \boldsymbol{r}_{ji} \circ \boldsymbol{u}_{ji}$; $T_{isj0} = -r_{ji}^{-3}\ \boldsymbol{r}_{ji} \circ \boldsymbol{u}_{is}$; $T_{isjt} = r_{ji}^{-3}\ \boldsymbol{u}_{isi} \circ \boldsymbol{u}_{jt} - 3r_{ji}^{-5}\ \boldsymbol{r}_{ji} \circ \boldsymbol{u}_{jts}\ \boldsymbol{r}_{ji} \circ \boldsymbol{u}_{iss}$, all indices refer to atom sites, the sums over 'j' omit $j=i$ terms, the $\boldsymbol{u}$'s are unit vectors determining the orientation of atom dipoles, and $\boldsymbol{r}_{ji} = \boldsymbol{r}_j - \boldsymbol{r}_i$. We calculate only the induced field and potential to obtain the induced charges and polarizations, ignoring the background charges present before the CT event. We do not include the partial charges that are already present on either the carbons or the nitrogen, e.g., in the CHARMM force field, aromatic carbons are assigned a charge of −0.115, and aromatic H's +.115, while aromatic nitrogens can have charges anywhere from −0.3 to −0.7. The charges we are dealing with are *induced* charges, and exist *in addition to* any background charges of this static nature.

Water molecules are then placed in the model at van der Waals + electrostatic potential energy minima about the rings, conformable to the point-group symmetry. Correspondingly, 16 waters surround the naphthalene and 11 surround the aniline (4 are hydrogen bonded to the nitrogen lone pair + amino protons—see Fig. 3B and C). The field due to the new charges was calculated, and the interaction energy was calculated according to

$$W_{\text{site–solv.}} = -\sum_i \mu_i \boldsymbol{E}(\boldsymbol{x}_i) + 1/2\alpha E^2(\boldsymbol{x}_i) + 1/3\Sigma_{\sigma\tau} Q_{\sigma\tau} \nabla \boldsymbol{E}_i, \tag{2}$$

(summing over sites, with all waters at a site treated separately, in the case of the anilino nitrogen, for example) where the μ is taken to be 1.84 D, the polarizability α is taken to be 1.444×10^{-24} cm^3, and the quadrupole moments $Q_{\sigma\tau}$ are taken from Stone [11]. The waters usually are oriented with the oxygen pointing directly to the hydrogen of a C–H site, since the additional charge, if any, on the carbon, plus the induced dipole moment there or on the proton, is usually not able to overwhelm the effect of the charge already present in the background, e.g., the CHARMM charges. Exceptions occur with the anilino nitrogen. Furthermore, the waters situated above the rings are able to reorient fairly easily (compared with those ostensibly H-bonded to carbon-bound protons). Thus, a large negative charge at the bridge-carbons of naphthalene will cause the waters located above and below the ring at the bridge positions to orient their protons toward them, to minimize the electrostatic potential. The calculation proceeded very much in the same manner as Bockris and Reddy's [12] calculation of hydration energies for single ions.

There are several possibilities with respect to the site-specific solvation. One 'minimal' model (1) would consist of removing three waters to "synthesize" the anilinonaphthalene, two from the four surrounding the aniline amino group, and one which is H-bonded to the naphthalene 1-C-H, the total "solvation energy" from this model is −103.8 (Born, naphth.)+−122.3 (Born, anil.)+−161.5 (site solvation)=−387.6 kJ/mol, which leads to an expected CT transition energy of 31140 cm^{-1}. Because of steric "crowding" at the 1-position in naphthalenes (the "peri"-effect, Ref. [13]), a second model (2) would envisage a loss of *three* waters from the anilino nitrogen and would lead to a CT transition energy of 33,060 cm^{-1}, or 302.5 nm. This can be compared with the transitions observed in aniline (280 nm), and in 1-anilinonaphthalene (265 nm and 303 nm), as well as in other anilinonaphthalenes (2,6-ANS; 1-anilino, 2-sulfo naphthalene, etc.). A third model (3) takes cognizance of the steric crowding possible between the C2′-H water of aniline and one of the waters lying above the plane of the naphthalene in the (anticipating a bit) major conformation in solution of the two rings, which are nearly orthogonal. Removing this water yields a transition energy of 35,730 cm^{-1}. These numbers are not meant to be taken as definitive, since there is a range of possible monopole and dipole polarizabilities to be employed. In addition, we calculated the dipole contribution to the induced electric potential on the rings only for nearest neighbors atoms, to reduce the number of off-diagonal terms in the matrix.

The excited state of aniline (An*) is close in energy to the CT state, as we know from Fig. 2. The two states–the aniline excited state with a naphthalene 'spectator'–{An*….Naphth}–and the CT final state–{An$^+$…Naphth$^-$}–are close in energy. So the zeroth-order energies of the aniline transition and the aniline–naphthalene CT transition will be perturbed from the values obtained as 'isolated species' by the electrostatic interaction H_{int} between the CT state dipole and the An* excited-state dipole. This is a common 'level shift' effect. Thus, we obtained 'first order' corrected energies of the *excited states*, from which we construct our *excitonic* states (below), via the solutions to the secular equation:

$$2E_{\pm}=E_1+E_2\pm[(E_1-E_2)^2+4H_{\mathrm{int}}^2]^{1/2} \tag{3}$$

1.3. Spectra 'mixing' methodology/exciton formalism

In this section, we wish to justify our employment of an excitonic formalism to manipulate the spectra. It would have been simpler to utilize the rotation matrix 'mixing' we employed in the previous paper, except for the fact that we are not dealing with two excited states on separate molecules, but rather with two nearly coincident excitations on *one*. In addition, the methodology requires there to be zero overlap, as we demonstrate below. The main idea of an exciton treatment is to employ a properly transformed version of the spectrum itself as a typical quantum state vector, and thereby subject it to various typical algebraic manipulations, such as orthogonalization and principal-axis transformation. An exciton is an electromagnetic field excitation localized in matter and is often viewed as an electron-hole pair; that is, a hole inserted into a ground-state orbital and an electron inserted into an excited-state orbital. The exciton possesses boson statistics, just like the captive photon it represents. Our plan is to perform manipulations on the absorption spectra themselves as if these energy distributions were a one-dimensional representation of ordinary wave vectors. We take the first-order synthetic spectra as above and remove the effects of their spatial overlap (re-orthogonalization), then proceed to take account of their remaining excitonic interaction by rotating them into stationary eigenvectors.

The underlying CT and aniline spectra are allowed to "mix", because of the following considerations: Suppose that the product of an excited-state operator with the ground-state wave function $\Psi^{\mathrm{ex}}{*}\Psi^{\mathrm{gr}}$ be integrated over the coordinates of all the electrons of the system but one. One then has a *transition density* ρ_{tr} such that $\int \boldsymbol{r}\rho_{\mathrm{tr}}\mathrm{d}^3\boldsymbol{r}$ is the transition dipole moment $\boldsymbol{\mu}_{\mathrm{tr}}$. The claim we make here is that the form above, having both real and imaginary components as a distributed function over space, has the quality of a wave function itself, and that it corresponds to the *exciton wave function*. This wave function then has the property that it possesses a continuous energy spectrum proportional to the distribution $\varepsilon(v)/v$ for absorbance and $f(v)/v^3$ for fluorescence. This follows since

$$\int \mathrm{d}t \int\int r'(t-t_0)\boldsymbol{A}(t)r(t_0))\boldsymbol{A}(t)\rho_{\mathrm{tr}}(t-t_0)\rho_{\mathrm{tr}}(t_0)e^{iEt/\hbar}\mathrm{d}^3r\mathrm{d}^3r' \tag{4a}$$

gives the integrated spectral intensity itself, or $I(\omega)$ (cf. Heller, 14), where $\boldsymbol{A}$ is the vector potential. Then, performing a Fourier transform with respect to space, into momentum coordinates first:

$$I(\omega)=\int \mathrm{d}tk'(t)k(t_0)\boldsymbol{A}^2\rho_{\mathrm{tr}}(t)\rho_{\mathrm{tr}}e^{i\omega t}\mathrm{d}^3k\mathrm{d}^3k'. \tag{4b}$$

With a new set of normalizations (cf. Bethe and Salpeter [15], converting $\mathrm{d}^3k\ \mathrm{d}^3k'$ to $\mathrm{d}E$), this is equivalent to (performing the Fourier time-integral)

$$\begin{aligned} I(\omega) &= \int \mathrm{d}E g_{\mathrm{k}}(k,\omega)(p_{\mathrm{tr,eff}}(\omega))^2 E_{\mathrm{field}}\rho_{\mathrm{tr,eff}}^2 \\ &= <p_{\mathrm{trf}}^2> \int E_{\mathrm{field}}\Phi(E)\mathrm{d}E = p_{\mathrm{tr,eff}}^2 \int E_{\mathrm{field}}\Phi(E)\mathrm{d}E \\ &= \sim \mu_{\mathrm{eff}}^2 \int v\Phi(v)\mathrm{d}v \end{aligned} \tag{4c}$$

where 'p_{eff}' is the effective transition momentum and $g_k(k,\omega)$ is the FT of a two-time correlation function of the transition momenta $k(t_0)$, $k'(t)$, so that $\Phi(E)$ is a probability distribution function [16,17] which yields the spectral density of the transition and is essentially the Frank–Condon weighted density of states (given by $\varepsilon(v)/(v\mu_{\mathrm{eff}}^2)$). As the exciton is supposed to be equivalent to a boson (even though it is made up of a product of fermion wave functions), we focus attention on the transition probability $\Phi(E)$ as the square of the transition density $\rho(\omega)_{\mathrm{tr,eff}}=\Psi_{\mathrm{a}}^{\mathrm{ex}}{*}\Psi_{\mathrm{a}}^{\mathrm{gr}}$; this expression is just as if this density were itself a transition *amplitude* that is, to make the transition density itself an exciton wave function, and the result of an exciton creation operator $\boldsymbol{A}^{\dagger}$:

$$\boldsymbol{a}'^{\dagger}\boldsymbol{a}=\boldsymbol{A}^{\dagger}, \tag{5a}$$

operating upon the ground-state electron density, or $\Psi_a^{\mathrm{gr}}{*}\Psi_a^{\mathrm{gr}}$ $\boldsymbol{A}^{\dagger}=\boldsymbol{A}^{\dagger}\rho_{\mathrm{gr}}$ where $\boldsymbol{a}'^{\dagger}$ is the *electron* creation operator for the |a′> excited electron-state (ket), and $\boldsymbol{a}$ is the *electron* annihilation operator for the |*a*> ground-state ket; similarly, one writes the exciton at '*b*' or $\Psi_b^{\mathrm{ex}}{*}\Psi_b^{\mathrm{gr}}$ as the result of

$$\boldsymbol{b}'^{\dagger}\boldsymbol{b}=\boldsymbol{B}^{\dagger} \tag{5b}$$

(with $\boldsymbol{b}'^{\dagger}$ and $\boldsymbol{b}$, the corresponding creation and annihilation operators). The $\boldsymbol{A}^{\dagger}$ ($\boldsymbol{B}^{\dagger}$) has to act on a system containing an electron in the ket |*a*> (|*b*>) to begin with. Conversely, exciton annihilating operators $\boldsymbol{A}$ and $\boldsymbol{B}$ can be defined as $\boldsymbol{a}^{\dagger}\boldsymbol{a}'$ and $\boldsymbol{b}^{\dagger}\boldsymbol{b}'$, respectively. The claim about the bosonic nature of the exciton is contained in the statements [18]

$$[\boldsymbol{A}^{\dagger},\boldsymbol{B}]=[\boldsymbol{B}^{\dagger},\boldsymbol{A}]=0. \tag{6}$$

A necessary condition for the first pair of commutators to vanish is that the *conjugate* commutator $\boldsymbol{A}^{\dagger}\boldsymbol{B}-\boldsymbol{B}^{\dagger}\boldsymbol{A}$ must be zero (or equivalently, $\boldsymbol{B}\boldsymbol{A}^{\dagger}-\boldsymbol{B}^{\dagger}\boldsymbol{A}$). Now, these must operate on different function spaces: $\boldsymbol{A}^{\dagger}\boldsymbol{B}$ requires a set |*a*, *b*',….> while $\boldsymbol{B}^{\dagger}\boldsymbol{A}$ requires |*a*′, *b*…> to operate upon. We have here an *excitation-transfer* operator. These product operators represent now an interaction between the two excitons and this interaction is *causal*, so we include a time dependence to the $\boldsymbol{A}$, $\boldsymbol{B}$ operators of the form $\mathrm{e}^{i\omega(A)t}$ for $\boldsymbol{A}^{\dagger}(t)$ and $\mathrm{e}^{-I\omega(A)t}$ for $\boldsymbol{A}(t)$, and similarly for $\boldsymbol{B}$ (with $\omega(A)$ and $\omega(B)$ the frequencies $E_{a(B)}/\hbar$), then we can make the coupled operators commute if we invoke the CPT theorem and if we are working at resonance between |*a*, *b*′> and |*a*′, *b*>. Nonetheless, there remains the requirement, after anticommuting the individual electron creation/annihilation operators, (cf. Ref [18]) both overlaps $(a'|b')$ and $(a|b)$ must = 0, where parentheses here imply spatial integration.

If one expands the previous commutators (in (6)), one finds one must meet the same overlap conditions as above except for the additional requirement that $(a'|b)$ and $(a|b')$ also vanish.

Now these two conditions are imbedded in one Gram–Schmidt orthonormalization process, because we expect the overlap of the ground states and that of the excited states to be related to each other by a proportionality constant. This orthonormalization removes the spatial overlap of $(a'b|b'a)$, and we have, now, a properly commuting pair of occupation operators.

Given one exciton state $|a'b\rangle = |\alpha\rangle$, say the first-order CT transition, we make the reorthogonalization:

$$\boldsymbol{A}\rightarrow\alpha = (a'^{*}a); \quad \boldsymbol{B}\rightarrow\beta = (b'^{*}b) - (\alpha|b'^{*}b)\alpha/||\alpha||^2 \tag{7}$$

Following Weyl [19], the energy overlap of the two excitons, though not extensive (even after our first-order corrections, because we have now transformed the excitons again by removing the effect of their spatial overlap, they are no longer necessarily diagonal), is enough to require us to transform to principle axes via a *quasiunitary* transform[1]:

$$\begin{vmatrix} H & \varepsilon \\ -\varepsilon & H \end{vmatrix} \begin{matrix} (\alpha) \\ (\beta) \end{matrix} \rightarrow \begin{vmatrix} 1 & \lambda H_0^{-1}\delta H \\ -\lambda H_0^{-1}\delta H & 1 \end{vmatrix} \begin{matrix} (\alpha) \\ (\beta) \end{matrix} \tag{8}$$

(cf. also Flanders [20]) so that the two new (diagonal) excitons can be written as

$$\int (\alpha|\alpha)\mathrm{d}E + 2(\alpha|\lambda H_0^{-1}\delta H|\beta)\mathrm{d}E + (\beta|\lambda^2 H_0^{-2}\delta H^2|\beta)\mathrm{d}E = \int A(E)\mathrm{d}E \tag{9a}$$

$$\int (\beta|\beta)\mathrm{d}E - 2(\beta|\lambda H_0^{-1}\delta H|\alpha)\mathrm{d}E + (\alpha|\lambda^2 H_0^{-2}\delta H^2|\alpha)\mathrm{d}E = \int B(E)\mathrm{d}E \tag{9b}$$

The term δH is the interaction Hamiltonian between the two excitons; we shall assume that it is of the form of a dipole–dipole interaction, the parenthesis indicating, again, spatial integration. The term $(\alpha|\alpha)\mathrm{d}E$ is then just $\Phi(E)\mathrm{d}E$ for the underlying (unperturbed) ‘a’ spectrum, and $(\beta|\beta)\mathrm{d}E$ is $\Phi(E)\mathrm{d}E$ for the corrected (orthogonalized) ‘b’ spectrum. The mixing variable ‘λ’ is then determined from the condition that

$$\int (\alpha|\beta)\mathrm{d}E + (\beta|\lambda H_0^{-1}\delta H|\beta)\mathrm{d}E - (\alpha|\lambda H_0^{-1}\delta H|\alpha)\mathrm{d}E - (\alpha|\lambda^2 H_0^{-2}\delta H^2|\beta)\mathrm{d}E = 0 \tag{9c}$$

This condition and the previous are equivalent to the position that the new states ought to be stationary (after rotation, the news states do not interact, so the off-diagonal terms are zero), similar to the development utilized in our previous contribution (*I*). The parameter λ now playing the part of the condition on $\tan(2\theta)$ of the previous paper.

The spatial overlap of the two excitons is separated into a radial and angular part, and further differentiated into $(a'|b')_{\mathrm{rad}}(a|b)_{\mathrm{rad}}$. The total number of electron-volumes the two ground states share is $\sqrt{8}/\sqrt{18}$. The angular part can be considered as involving the ascent from the $\mathbf{D}_{6h} \supset \mathbf{C}_{2v}$ symmetry of aniline to $\mathbf{SO}_3$ the angular momentum group for a single electron, and the descent to $\mathbf{D}_{2h}$ again (where $\mathbf{SO}_3 \supset \mathbf{D}_\infty \supset \mathbf{D}_{6h} \supset \mathbf{D}_{4h} \supset \mathbf{D}_{2h} \supset \mathbf{C}_{2v}$ is the complete chain). The momentum of the compound (exciton) state of the CT $(a'b)$ is either 2 or 0, because of the $3-j$ symbol:

$$\begin{pmatrix} 1 & k & 1 \\ 0 & 0 & 0 \end{pmatrix} \text{appearing at the } \mathbf{SO}_3 \rightarrow \mathbf{D}_\infty \text{ level}$$

(cf. [5]; also [21]).

The angular momentum of the aniline can be expected, on the grounds of Hueckel-level MO theory, to be $E_{2u} \times E_{2u}$ $(= |2\rangle + |0\rangle + |0\rangle$ in Butler’s ‘natural’ system which descends in symmetry to ‘$|0\rangle$’ in C_{2v}), and $A_u \times B_{1g} = B_{1u} = |0\rangle$ in the natural system, for naphthalene. With ‘k’ equal to ‘2’ for the CT transition, the above $3-j$ symbol equals $\sqrt{2/15}$, while for ‘k’ = 0, it is $-1/\sqrt{3}$.

Another angular momentum factor arises because the two rings are not coplanar. A definite change in the direction of the axis *normal* between the two rings implies that the angular quantum number m_j for the z-axis (the *normal*) is not well defined, but that a Wigner rotation matrix for the $l = 1$ case must be specified. If we take the anilinonaphthalene structure to be determined by three consecutive rotations about two orthogonal axes (which we can place in the naphthalene ring-plane), we can suppose at first that the two rings are in the same plane, with the $\mathrm{C1_{napth}{-}N{-}C1'_{anil}}$ bonds defining one axis. Then rotation by θ about this axis, rotation by ϕ about the axis parallel to the long axis of naphthalene *through the N atom*, followed by rotation about the first axis of the ‘paddle’ we have just created, will unambiguously map any two conformers of the two rings. The matrix element for the first and last rotation depends on the m_j values, which we argue are confined to ‘0’, hence, rather surprisingly, there is no contribution to the matrix element from these ring-reorientation movements (cf. [22]). They would otherwise present themselves as phase factors $e^{im\phi}$. The second rotation is, of course, the relative bond angle of the C–N–C bond. But this rotation really represents the degree to which the nitrogen *lone pair* is brought out of the perpendicular, so we assume that its maximum value is 30°—since in the CT state we

---

[1] One should note the similarity with the rotation matrix used in the previous contribution. In fact to make the transform exactly unitary, one need only divide each entry of 7 by $\sqrt{(1+\eta^2)}$ where η is $\lambda H_0^{-1}\delta H$. If we imagine η to be strictly real, then it is the tangent of some angle θ, and the ordinary rotation matrix is, in fact, recovered. More interestingly, if η is *complex* then one still has an orthogonal transform, but now with a complex angle—hence the name *quasiunitary*. Eq. (7) is given to motivate the change from a form of interaction matrix with which many readers will be familiar, to the ‘rotation’ form. Moreover, Flanders [20] discusses the $A^{-1}\mathrm{d}A$ as a infinitesimal translation/rotation operator, which motivates our use of the coupling parameter λ in order to produce a finite translation of the exciton wave vectors toward the perturbing vector. The use of δH is to remind us that the matrix elements are *functionals* of the space coordinates, while they are *functions* of the energy.

have nearly a whole electron lost to the aniline carbon, and the remaining electron is in an extended π∗ bond. Thus, the Wigner rotation gives us a contribution of cos30° at most. The $3-j$ symbol to $\mathbf{D}_\infty$ has a value of $1/\sqrt{3}$, the other ones occurring further down the group 'chain' having a value of 1.00.

The lone pair at 'N' can be occupied or not by both electrons in the transitions. So the radial overlap would be $\sqrt{(1+g_{\mathrm{CT}})}\sqrt{(1+g_{\mathrm{anil}})}=1+g_{\mathrm{eff}}$ for this position, where the g's represent degrees of electron correlation in space at the 'N' center, and a full pair has $g=1$. For the rest of the electron volumes of the transition, there is a direct overlap of $1/(\sqrt{7}\sqrt{11})$. If we assume g_{eff} is about 0.4–0.6, we obtain a total overlap of 0.04–0.16.

The spectrum is generated from re-orthogonalized excitons, together with the underlying dipoles according to the following formulas:

$$\begin{aligned}\boldsymbol{\mu}_{tr,A} &= \phi(a)\boldsymbol{\mu}_a + 2\lambda\langle H_{\alpha\beta}\rangle/H_0\phi(a)^{1/2}\phi(b)^{1/2}\langle\alpha|\boldsymbol{\mu}|\beta\rangle \\ &\quad -2\lambda^2\langle\alpha|\beta\rangle\langle H_{\alpha\beta}\rangle^2\phi(\beta)\boldsymbol{\mu}_b\end{aligned} \tag{10a}$$

and

$$\boldsymbol{\mu}_{\mathrm{tr},B} = \phi(b)\boldsymbol{\mu}_b-2\lambda\langle H_{\alpha\beta}\rangle/H_0\phi(a)^{1/2}\phi(b)^{1/2}\langle\alpha|\boldsymbol{\mu}\beta\rangle. \tag{10b}$$

where $\boldsymbol{\mu}_a$ is the transition moment for the underlying CT transition, $\boldsymbol{\mu}_b$ is that for the aniline, and the $(\alpha|\boldsymbol{\mu}|\beta)$ is the transition moment between the two excited 'states'. The value of $\boldsymbol{\mu}_a$ was chosen to be consistent with the spectra of several anilinonaphthalenes, to be 5D. For aniline, the UV absorbance spectrum of aniline in water was used, together with the well-known relationship (cf. [23]):

$$\begin{aligned}\langle\boldsymbol{\mu}_{tr}\rangle^2 &= (3000\ln 10hc/8N_{0^{\pi^3}})\int \varepsilon(v)/v\ \mathrm{d}v \\ &= 9.18\times10^{-3}\int \varepsilon(v)/v\ \mathrm{d}v \text{ in } (\mathrm{esu{-}cm})^2.\end{aligned} \tag{11}$$

The $\langle H_{\alpha\beta}\rangle$ matrix element is calculated from the transition dipoles for the CT and aniline excitons (the dipole–dipole interaction of the excitons is that between the transition dipoles of the underlying single electron states) as

$$\langle H_{\alpha\beta}\rangle = -\boldsymbol{\kappa}\mu_a\mu_b/R^3 \tag{12a}$$

where κ is the (diagonal) dipole–dipole orientation tensor:

$$\kappa = \{\boldsymbol{u}_{\mathrm{trp}}\circ\boldsymbol{u}_{\mathrm{ans}}-3(\boldsymbol{u}_{\mathrm{trp}}\circ\boldsymbol{R})(\boldsymbol{u}_{\mathrm{ans}}\circ\boldsymbol{R})/\boldsymbol{R}^2\}, \tag{12b}$$

and the $\boldsymbol{u}$'s are unit direction vectors, with $\boldsymbol{R}$ the separation vector between the dipoles μ.

2. Materials and methods

1,8-Aminonaphthalene sulfonate (AmNS) was obtained from Pfaltz and Bauer (Waterbury, CT) and was recrystallized from boiling MeOH–H_2O into which 2 mls/50 g of concentrated $NH_3{\cdot}H_2O$ was added. A similar procedure (without the ammonia) was used to recrystallize 1-anilinonaphthalene (AnN), also from Pfaltz and Bauer. ANS was as previously described [24,25]. The other ANS congeners employed (1,2-ANS, 2,1-ANS, 2,6-ANS, and 2,8-ANS) were obtained from Molecular Probes and used directly. Dimethylformamide (DMF), cyclohexane (CH), acetonitrile (MeCN), and tetrahydrofuran (THF) for use as solvents in Stokes shift analysis were obtained from Burdick and Jackson (Muskegon, Michigan) and used fresh. Aniline was from Acros (New Jersey).

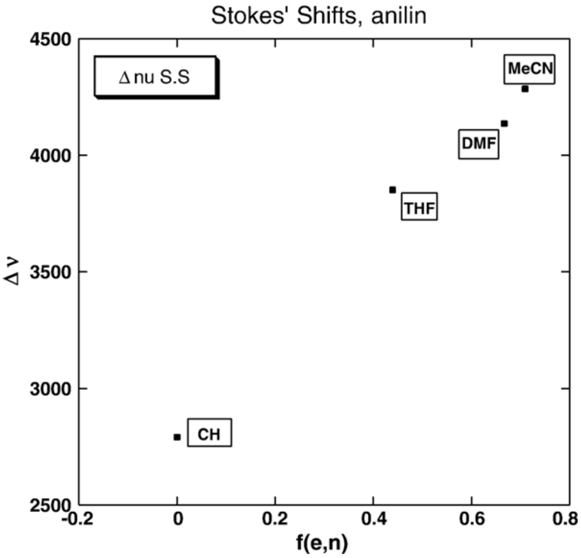

Fig. 4. Stokes shifts (Δv) in cm^{-1} for the solvents as labelled, versus the solvent function $f(\varepsilon, n)$ defined in Eq. (12b). CH = cyclohexane. THF = tetrahydrofuran. MeCN = acetonitrile, DMF = dimethylformamide.

Absorbance (CD) spectra were collected as previously described ([24], also in *I*).

The *excited state dipole moment* (used in the H_{int} for the 'level shift' calculation) of aniline is derived from a Lippert–Matanaga–Ooshika [26] analysis of the Stokes shifts of aniline in various dipolar–aprotic solvents.

$$hc\Delta v_{\mathrm{Stokes}} = 2f_{\mathrm{solv}}/a_0^3(\mu_{\mathrm{F}}(\mu_{\mathrm{F}}-\mu_{\mathrm{I}}) \quad \text{where } f_{\mathrm{solv}} \text{ is the function} \tag{13a}$$

$$(\varepsilon_{\mathrm{s}}-1)/(\varepsilon_{\mathrm{s}}+2)-(n^2-1)/(n^2+2) \text{ for each solvent,} \tag{13b}$$

with μ_{I} being taken to be 1.13D, and a_0 being the Onsager cavity radius, for aniline ~4.9 Å. For this analysis, we used the solvents as described in the Fig. 4. The static dipole moment of the CT-final state of anilinonapthalene was taken to be as calculated from the partial charges generated by the Applequist model (as above in Section 1).

3. Results and discussion

The charge distribution found from the Applequist model for naphthalene and aniline are shown in Fig. 3B and C. For anilinonaphthalene, we can take the second model of site hydration and expect that the unmixed CT transition should occur at 33,060 cm^{-1}, with aniline in H_2O having its transition at 35,714 cm^{-1}. From the slope of the Stokes shifts (Fig. 4), and the ground-state dipole moment of aniline of 1.13 D [27], we calculate an excited-state dipole for aniline of 2.33 D, and

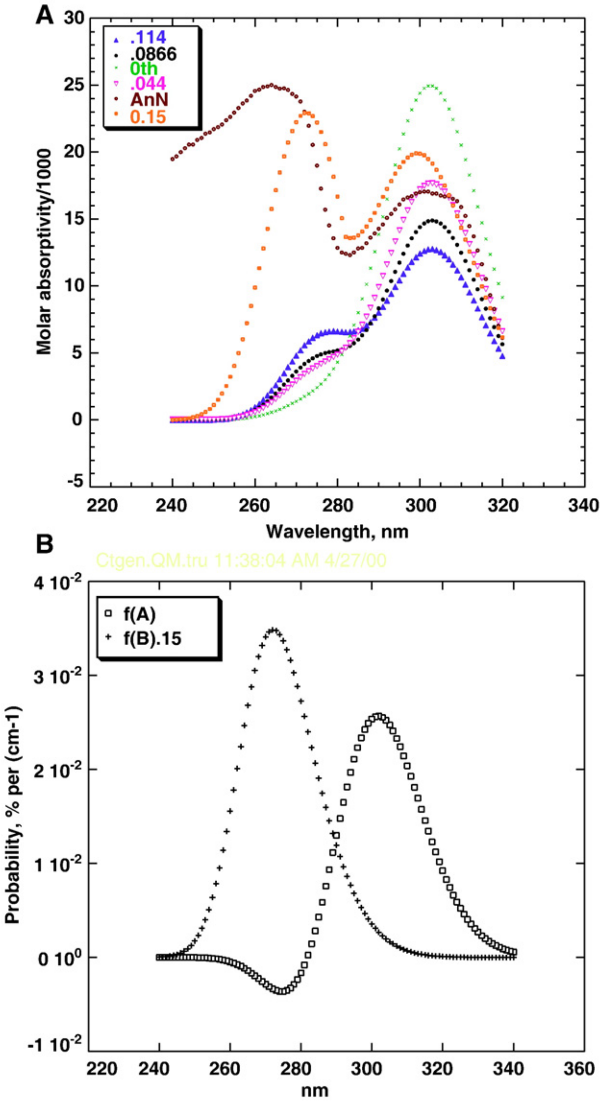

Fig. 5. (A) Anilinonaphthalene (AnN) spectrum and derived spectra. The original first-order spectrum for the CT is shown as the large unstructured band at 299 nm. We illustrate also the effect of different possible values for overlap, with values of 0.044, 0.0866, 0.114 and.0.15 (see text) on the final 'derived' spectrum (which uses 0.15 for overlap, and the quasiunitary principle axis transformation, and an improved choice for the $<\alpha|\boldsymbol{\mu}|\beta>$, i.e., as given in the text). Note the 3-nm shift induced by this transformation. For comparison, we also show the AnN spectrum again. (B) The component excitons $f(A)$ and $f(B)$ for the final derived spectrum for AnN. The original 'a' and 'b' spectra are normalized Gaussians with 1700 cm^{-1} and 1500 cm^{-1} widths, respectively.

thence, we calculate an interaction energy $\langle H_{\mathrm{int}}\rangle$ between the static excited-state dipoles of 2700 cm^{-1} with 7.12 Å separation of the centers. The anilinonaphthalene dipole moment in the CT state is given by (1.4705, 3.0016, −1.7487) in e_0-Å. As a check on the Applequist model, we construct the anilinonaphthalene, and calculate the $\boldsymbol{E}$ field produced by the above dipole moment, and then go through another round of polarization. The resulting charges are only trivially different from those calculated on aniline and naphthalene in the absence of the excess field (i.e., only distributing the excess charge on each separate subunit).

We write the expected (first order) energies of the states for anilinonapthalene from Eq. (3) which follows from solving the secular determinant for the effect of H_{int} on the zeroth-order energies. For the given values one obtains $E_+=37{,}531$ cm^{-1}, and $E_-=31{,}243$ cm^{-1}. These energies are then the maxima of two Gaussian distributions from which the $|\alpha>$ and $|\beta>$ excitons are constructed. We found our best fitting to total spatial overlap of about 0.15. Less than this value, and the AnN spectrum cannot be closely approximated. This value is at the high range of what we had deemed *a priori* was a physically reasonable value.

For ANS, we made the assumption that the underlying zeroth-order CT would be centered at the value of 35,730 cm^{-1} (cf. Section 1.2). Then the first-order states (from Eq. (3)) are centered at 38,422 and 33,022 cm^{-1}. Figs. 5 and 6 show what happens to the two transitions, under the assumption of three vs four waters missing from the anilinonaphthalene complex, after mixing the excitons. We have also generated the underlying

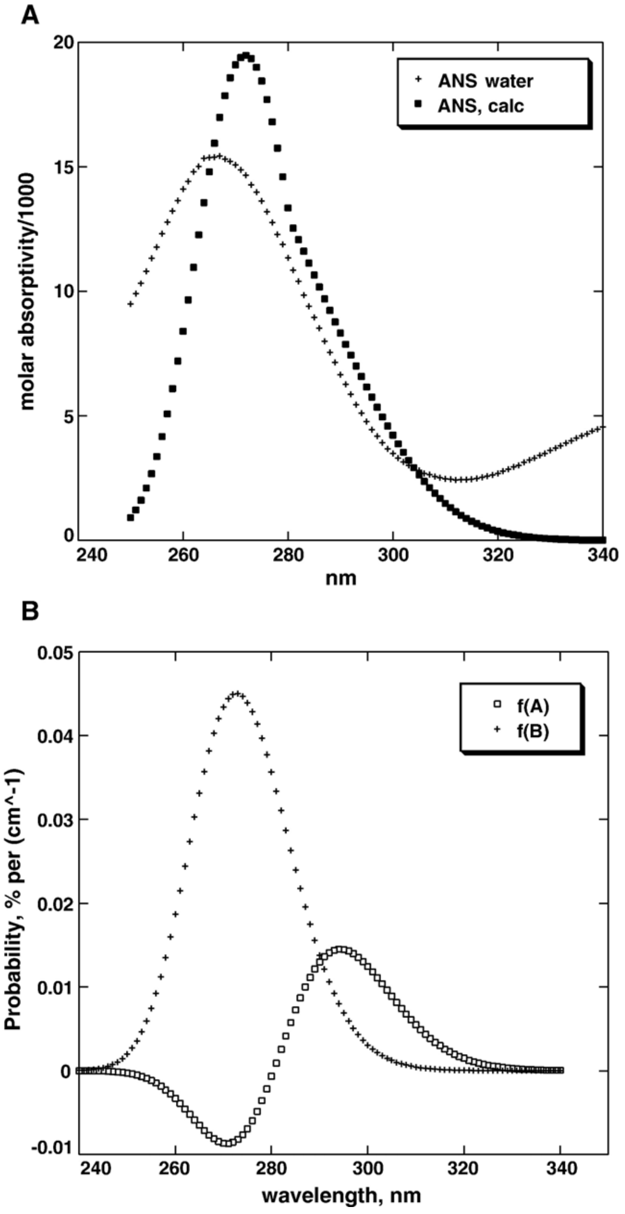

Fig. 6. (A) 1,8 ANS spectra, as with Fig. 5. (B) Component excitons. Note the far larger component of $f(A)$ that is 'antisymmetric,' compared with AnN.

excitons (Figs. 5B and 6B) as functions of energy from the spectra. There are two more fitting parameters to be specified: the transition moment $(\alpha|\boldsymbol{\mu}|\beta)$ between the now coupled excitons. So with two parameters μ_x and μ_y, one fits the spectrum of anilinonaphthalene, and for a different choice, fits that of ANS (cf. Eqs. (10a) and (10b)). Parenthetically, one can without too much prejudice assume that both transition vectors do lie in the same plane, since they have one terminus, namely, the anilino nitrogen, or the C1′ carbon, in common, at least for the case of AnN. The between-excited-state transition dipoles chosen are located at (6.33, 11.06) for AnN and (6.7, 10.99) for ANS, leading eventually to transition dipoles for the '*A*' and '*B*' spectra of (3.305, −3.06) and (0.809, 3.596) for AnN '*A*' and '*B*', respectively, and (2.037, −1.69) and (2.25, 2.0988) for ANS. These latter values are, it should be emphasized, *derived*, given only the terms we have used and chosen (above) for the between-excited-state transition moments, and the other parameters as determined from the techniques employed in this paper. As one can note, the presence of the sulfonate seems to 'rotate' the '*B*' spectrum dipole moment toward the sulfonate, whereas it effectively only scales back the '*A*' moment. This result was neither presumed nor even anticipated, we reiterate, notwithstanding it seems to make a great deal of physico-chemical sense. Figs. 5 and 6 demonstrate the similarity of our derived $A+B$ spectra for AnN and ANS with the original spectra (cf. Fig. 2C). The value for the excited state dipole moment of aniline (1.15 D) is subject to the error in the Lippert plot, about 8%. The error in choice of between-exciton transition dipole for AnN and ANS is probably larger, we have given our choice of values, which contributes to the derived value of the first transition dipoles (i.e., from the ground state) for the *A* and *B* excitons via Eqs. (10a) and (10b). These values could be in error by a large margin, since they are essentially guesses. Nonetheless, the final dipole moments seem to be accurate to ~16%, since at most the derived ANS molar absorptivity is within 33% of the observed. The error in energies are mostly to be expected in site solvation energy and in the dipole–dipole interaction energy. They can be estimated to account for a possible error of about 1100 cm^{-1} (~13 kJ/mol–8% of site solvation, roughly one water) and 300 cm^{-1} (10% of H_{in}–8% from error in the Lippert slope and 6% from $1/r$ values treated as independent errors), respectively. The energy we calculate for the '*B*' spectrum of ANS is in fact about 688 cm^{-1} and for AnN is about 1200 cm^{-1} too small. If there were an additional 'level shift' due to the partially 'hydrophobic' pocket in which aniline finds itself in the 'compound' anilinonaphthalene, relative to pure water, this could shift the 'zeroth'-order spectrum of aniline to the blue. We have no unambiguous, quantitative way of introducing such a correction into our analysis, though it seems reasonable that such a shift might occur. The observed AnN spectrum is further complicated by the fact that its '*B*' spectrum is located on the downward slope of a much stronger transition at higher energy (ca. 220 nm). Both '*A*' spectra seem to be fairly well captured, however.

There is an increase in the integrated $^1\text{L}_\text{a}$ intensity in ANS relative to AnN, but that difference is relatively small, compared to the change in the integrated intensity from 250–320 nm, from AnN to ANS. There is also, admittedly, an increase in the $^1\text{L}_\text{a}$ transition density in the FABP-bound ANS, relative to H_2O solution, so, presumably some of this borrowing from the CT+ aniline transition accommodates some of the loss of integrated intensity suffered by ANS in that region for the bound species.

In low water-activity solvents, the absorption spectrum of ANS displays an enhanced red peak ~370 nm., cf. Fig. 9b in Ref. [6]. This is also apparent in the protein systems displayed therein. The appearance of this peak is also correlated with enhanced fluorescence quantum yield and lifetime in protein or solvent systems.

It is rather unexpected that the site hydration energy for naphthalenide anion is essentially zero, when that for anilinium is so large. But it will be observed that the excess charge is fairly broadly distributed around the ring in naphthalene, and contrariwise, in the case of anilinium, it is fairly concentrated at the nitrogen and C1′ carbon. Further, in naphthalene, there is a good chance that the C–H bond dipole can repolarize and compensate much of this charge, whereas in aniline, the C1′ does not have a polarizable C–H bond, and the nitrogen is directly exposed to water. Put another way, the carbons of naphthalene have a mediating proton between them and the water, which aniline does not. Of course, each charge in the case of naphthalene is only −.3, as opposed to +.6 and +.5 for aniline.

We take up the differences in fluorescence quantum yield, especially with respect to a putative electron transfer to solvent quenching mechanism in a later contribution (also addressed in Ref. [6], however). But for now, we wish to note the correlation of Stokes shift in fluorescence with 'solvent reorganization' energy. This correlation, in fact more of an identity than a mere correlation, is also responsible ultimately for the difference in quantum yield of the hydrated ANS versus AnN. But the sulfonate quite possibly directs water dipoles against an electron-in-solvent, whereas the positive pole on the Nitrogen from the CT state, by itself, would tend to orient water dipoles *toward* an electron in solvent: especially if the electron had a high probability to emerge on the aniline side of the naphthalene (i.e., towards the 1,8 end and away from the 4,5 end). Hence, there would be less solvent reorganization energy required for AnN than for ANS for electron transfer to solvent, while it is an observed fact that there is less of a Stokes shift for the fluorescent state for AnN than for ANS. It would seem that there must be some borrowing of the naphthalene excited state from the CT state to account for this agreement—i.e., the fluorescent state of both AnN and ANS seems to share some of the character of the CT state, notwithstanding that the identity of the fluorescing state is L_a of naphthalene. In water, possibly because of the proximity of the nearest approach of the solvent dipoles and possibly because the solvent is less 'preordered' for the fluorescent/electron transfer state charge distributions by the original ground-state distributions (not mutually exclusive considerations), the Stokes shift/reorganization energy is maximal, while in larger, less protic solvents such as acetonitrile there is much more 'pre-ordering' of the solvent, and less of a Stokes shift/solvent reorganization energy (cf. Part V).

The Applequist polarizability model we employed to generate our 'CT' structure, is of course essentially a classical model. There is also a range of values for the monopole and dipole polarizabilities which might have been employed in determining the CT charge distribution. We chose values in the center of each range. We also made no attempt to find the 'global minimum' of the gas-phase electrostatic models with 11 and 16 waters, respectively, via a molecular mechanics algorithm, for example. We simply chose reasonable geometries consistent with known chemistry—i.e., van der Waals minima, etc. A full-scale calculation with a large number of waters may be worth attempting, but there is no guarantee that any models for 'computer water' readily available would be consistent with the polarization approach employed here, though certain alternatives are conceivable (*vide infra*).

There is another problem with the approach we used: we did not solve the full Applequist model, rather, the dipole contributions to the ***E*** field at each point were restricted to only nearest neighbor effects. In fact, this may not be such a serious error—because of both the point group symmetry and Gauss' law, one may expect that any modification in the density of lines of electric force must be the same in each octant of the naphthalene coordinate system, and each quadrant of the aniline, respectively, so that whatever field perturbation may be suffered by one water, due to neglected polarizations, the effect on the total interaction energy is probably compensated by the effect on other waters, especially out at the radial distance where the waters are actually located—since the sum of all lines of force in each sector must be constant. These caveats aside, the Applequist approach would seem to be a very promising for generating *a priori* predictions of CT spectra. One can envision a Monte Carlo-based simulation with a large number of surrounding waters, and some such model as Barnes et al.'s [28] 'polarizable electropole', Millot and Stone's [29] polarizable water model, or else the Stillinger and David [30] 'polarization' model, to calculate the effective site-hydration energy, as a refinement to this model. For that matter, high-level quantum mechanical studies, either of the MO or density functional variety, possibly including bound waters, might be employed to further refine our understanding of ANS photophysics, beyond the Applequist model used here. This contribution is intended as a step in this direction.

Acknowledgement

This work was supported by NIH grant GM34847 to Franklyn G. Predergast, in whose laboratory this work was performed.

References

[1] G. Rodionova, N. Razgulyaev, O. Uversky, V. Gripas, V. Gilmanshin, Study of the Molten Globule intermediate state in protein folding by a hydrophobic fluorescent probe, Biopolymers 31 (1991) 119–128.

[2] J. Slavik, Anilinonaphthalene sulfonate as a probe of membrane composition and function, Biochim. Biophys. Acta 694 (1982) 1–25.

[3] P. Callis, ^1L_a and ^1L_b transitions of tryptophan: applications of theory and experimental observations to fluorescence of proteins, Methods Enzymol. 278 (1997) 111–150.

[4] G. Berden, W. Meerts, D. Plusquellic, I. Fujita, D. Pratt, High resolution electronic spectroscopy of 1-aminonaphthalene: S_0 and S_1 geometries and $S_1 \leftarrow S_0$ transition moment orientations, J. Chem. Phys. 104 (1996) 3935–3946.

[5] P. Butler, Point Group Symmetry Applications, Plenum Pr., N.Y., 1981

[6] W. Kirk, The binding of ANS congeners to I-FABP and comparison of some hypotheses about ANS' spectral sensitivity to environment, Biochim. Biophys. Acta 1748 (2005) 84–93.

[7] R. Mulliken, Molecular compounds and their spectra, J.A.C.S. (1952) 811–824.

[8] H. Zollinger, C. Wittwer, Grundlagen der Wirkung von Sulfamid-und Methylsulfongruppen in Farbstoffen: *Hammett's* σ*-*Werte und Solvationseffekte, *Helv. Chim. Acta*, 39 *Fasciculus II*, (1956) 347–356., also references therein.

[9] S. Murov, I. Carmichael, G. Hug, Handbook of Photochemistry, 2nd Edition. Marcel Dekker, N.Y., 1993.

[10] J. Applequist, Atom charge transfer in molecular polarizabilities, Application of the Olson–Sundberg model to aliphatic and aromatic hydrocarbons, J. Phys. Chem. 97 (1993) 6016–6023.

[11] A.J. Stone, The theory of intermolecular forces, Int. Ser. Monogr. Chem. 32 (1996) (Oxford U. Pr.).

[12] J. Bockris, A. Reddy, Modern Electrochemistry, Plenum Pr., N.Y., 1975

[13] V. Balasubramaniyan, *Peri*-interactions in naphthalene derivatives, Chem. Rev. 66 (1966) 567–641.

[14] E. Heller, The semiclassical way to molecular spectroscopy, Accounts Chem. Res. 14 (1981) 368–375.

[15] H. Bethe, E. Salpeter, Quantum Mechanics of One- and Two-Electron Atoms, 1957, Plenum Pr. N.Y. edition (1977).

[16] G. Schatz, M. Ratner, Quantum Mechanics in Chemistry, Dover Publ. Mineola, N.Y., 2002, pp. 201–214.

[17] D. McQuarrie, Statistical Mechanics, University Sci. Sausalito, 2000, pp. 553–572.

[18] P. Jørgenson, J. Simons, Second Quantization-Based Methods in Quantum Chemistry, Acad. Pr., N.Y., 1981.

[19] H. Weyl, The Theory of Groups and Quantum Mechanics, 1950, Dover ed. N.Y.

[20] H. Flanders, Differential Forms with Applications to the Physical Sciences, 1963, 1989 Dover edition, pp. 35–37.

[21] B. Judd, Operator Techniques in Atomic Spectroscopy, McGraw-Hill, N.J., 1963, pp. 70–73.

[22] A. Edmonds, Angular Momentum in Quantum Mechanics, Princeton Univ. Pr., N.J., 1960.

[23] C. Cantor, P. Schimmel, in: Biophysical Chemistry, 1980, Freeman, N.Y. pp Jackson, J, (1975) Classical Electrodynamics, 2nd ed. J. Wiley and sons, N.Y.

[24] W. Kirk, E. Kurian, F. Prendergast, Characterization of the sources of protein–ligand affinity: 1-sulfonato-8-anilinonaphthalene binding to intestinal fatty acid binding protein, Biophys. J. 70 (1996) 69–83.

[25] E. Kurian, Solution Structure of Intestinal Fatty Acid Binding Protein complexed with 1-Anilinonaphthalene-8-sulfonate: Implications for Ligand Binding, 1998, Thesis, Mayo Graduate School of Medicine, Rochester Minn.

[26] Y. Ooshika, Absorption spectra of dyes in solution, J. Phys. Soc. Jpn. 9 (1954) 594–605.

[27] K. Hellwege, Landolt–Boernstein, Numerical Data and Functional Relationships in Science and Technology, Group II, 14,a, Springer-Verlag, Heidelberg, 1982.

[28] P. Barnes, J. Finney, J. Nicholas, J. Quinn, Cooperative effects in simulated water, Nature 282 (1979) 459–464.

[29] C. Millot, A. Stone, Towards an accurate intermolecular potential for water, Mol. Phys. 77 (1992) 439–462.

[30] F. Stillinger, C. David, Polarization model for water and its ionic dissociation, J. Chem Phys. 69 (1978) 1473–1485.